Event-triggered Boundary Control of Mixed-autonomy Traffic

Yihuai Zhang, Huan Yu*

***Abstract*— Control problems of mixed-autonomy traffic system consisting of both Human-driven Vehicles (HV) and Autonomous Vehicles (AV) have gained increasing attention. This paper is focused on suppressing traffic oscillations of the mixed-autonomy traffic system using boundary control design. The mixed traffic dynamics are described by a 4×4 hyperbolic partial differential equations (PDE) which governs propagation of four properties in traffic including density of HV, density of AV, friction between two classes of vehicles from driving interactions, and averaged velocity. We propose event-triggered boundary control design since control signal of traffic light on ramp or varying speed limit cannot be updated in a continuous time fashion. We apply event-triggered mechanism for a PDE backstepping controller and obtain dynamic triggering condition. Lyapunov analysis is conducted to prove the exponential stability of the closed loop system with the event-triggered controller. Numerical simulation demonstrates how car-following spacing of AV affects event-triggering mechanism of control input in mixed-autonomy traffic.**

I. INTRODUCTION

Various boundary control designs have been studied for suppression of freeway traffic congestion [15]. The practical implementation of boundary control signal is via traffic light on ramp and varying speed limit (VSL). With the fast development of autonomous driving technology, the penetration of autonomous vehicles (AV) in traffic has increased over the past years, leading to a mixed-autonomy traffic system consisting of both human-driving vehicles (HV) and AV. Traffic oscillations could be induced due to car-following and lane-changing interactions between AV and HV. The design of boundary control strategies for mixed autonomy traffic remains an open question.

Event-based control is a computer control strategy which aims to improve efficiency of a system by updating the controller aperiodically. It needs to define a triggering condition for the system to determine the time instant that the controller need to be updated. The triggering condition can be both static and dynamic [16], [6]. Event-triggered control for hyperbolic PDEs was first developed by Espitia [4]. A continuous control input that can stabilize the system is first developed with an event-triggered mechanism embedded in the system. The event-triggered mechanism is executed based on the system states and the state describing the dynamics of the mechanism. Then the event-triggered control input that can also stabilize the system is obtained through the mechanism. With applications in traffic, Yu [18] first got the results for stabilizing the traffic oscillations using backstepping method with both theoretical guarantee and application possibility. The author in [3] developed the event-triggered output-feedback controller for cascaded roads. The event-triggered boundary controller created a more realistic setting to implement for traffic management system. Event-triggered control has gain a lot of interests due to its efficient way to use communication and computational resources by updating the control value aperiodically.

The traffic dynamics for pure HV traffic are described by hyperbolic PDEs such as first-order Lighthill and Whitham and Richard (LWR) model [11], [14], and the second-order Aw-Rascle-Zhang (ARZ) model [1], [19]. They are both continuous traffic models. Backstepping boundary control has been developed for the ARZ model [18], [17], [3]. Besides backstepping control method, feedback control [10], [20], optimal control [7], [8] can be also applied for boundary stabilization of traffic PDE models. Boundary control input is implemented by manipulating red-green phase of traffic lights on ramp and velocity display of VSL. The continuous control input is needed to update periodically at each time step which makes it hard to implement. Some work built on emulation of ramp metering controllers for discrete-time traffic system and designed discrete control law. The author in [13] proposed a hierarchical centralized/decentralized event-triggered control method for multi-class traffic networks modeled by METANET to reduce the computation and communication load. Ferrara [5] introduced the event-triggered model predictive schemes of discrete model for freeway traffic control.The event-triggered MPC triggering condition is a simple logic rule and is only for the discretized model. However, previous results for mitigating traffic congestion are mainly focused on traffic consisiting only HV. For the mixed-autonomy traffic, interactive driving behaviors of AV and HV on the road can make boundary control problem more challenging. Mohan [12] proposed a two-class traffic PDE model by introducing the concept of area occupancy to capture interactions between different classes. Burkhardt [2] adopted the two-class traffic PDE model and developed an output-feedback boundary controller using the backstepping method to get exponential stable results in L_2-sense. In this paper, we proposed the event-triggered control method for the mixed-autonomy traffic system.

The main contributions of this paper lie in two parts: On the one hand, we first propose the event-triggered controller for the mixed-autonomy traffic system modeled by an extended ARZ model and provide the theoretical guarantee using Lyapunov analysis. On the application side, the results can be applied to traffic management systems to reduce

Yihuai Zhang and Huan Yu are with the Hong Kong University of Science and Technology (Guangzhou), Thrust of Intelligent Transportation, Guangzhou, Guangdong, China. Huan Yu is also affiliated with the Hong Kong University of Science and Technology, Department of Civil and Environmental Engineering, Hong Kong SAR, China.

* corresponding author (huanyu@ust.hk).

computational resources and improve the efficiency of the traffic system. It paves the way for traffic management.

The paper is organized as follows. Section 2 introduces the mixed-autonomy traffic system using the extened-ARZ model. In Section 3, the boundary control model is derived and the backstepping controller with a continuous version is proposed. In Sections 4, the dynamic event-triggered condition is given and thus the event-triggered boundary controller is developed then the Lyapunov analysis is conducted to analyze the stability of the closed-loop system. Section 5 provides the numerical simulation results to verify the theoretical results. Section 6 goes to the conclusion.

II. Mixed-autonomy Traffic PDE Model

Motivated by the two-class extended ARZ PDE model [2], the mixed-autonomy traffic consisting of HV and AV is proposed as

$$\partial_t \rho_{\mathrm{h}} + \partial_x \left(\rho_{\mathrm{h}} v_{\mathrm{h}}\right) = 0, \tag{1}$$

$$\partial_t \left(v_{\mathrm{h}} - V_{e,\mathrm{h}}\right) + v_{\mathrm{h}} \partial_x \left(v_{\mathrm{h}} - V_{e,\mathrm{h}}\right) = \frac{V_{e,\mathrm{h}} - v_{\mathrm{h}}}{\tau_{\mathrm{h}}}, \tag{2}$$

$$\partial_t \rho_{\mathrm{a}} + \partial_x \left(\rho_{\mathrm{a}} v_{\mathrm{a}}\right) = 0, \tag{3}$$

$$\partial_t \left(v_{\mathrm{a}} - V_{e,\mathrm{a}}\right) + v_{\mathrm{a}} \partial_x \left(v_{\mathrm{a}} - V_{e,\mathrm{a}}\right) = \frac{V_{e,\mathrm{a}} - v_{\mathrm{a}}}{\tau_{\mathrm{a}}}, \tag{4}$$

$\rho_{\mathrm{h}}(x,t)$ and $\rho_{\mathrm{a}}(x,t)$ are the traffic densities of HV and AV, $v_{\mathrm{h}}(x,t)$, $v_{\mathrm{a}}(x,t)$ are the traffic velocities of HV and AV. The boundary conditions are set as

$$\rho_{\mathrm{h}}(0,t) = \rho_{\mathrm{h}}^{\star}, \tag{5}$$

$$\rho_{\mathrm{a}}(0,t) = \rho_{\mathrm{a}}^{\star}, \tag{6}$$

$$\rho_{\mathrm{h}}(0,t) v_{\mathrm{h}}(0,t) + \rho_{\mathrm{a}}(0,t) v_{\mathrm{a}}(0,t) = \rho_{\mathrm{h}}^{\star} v_{\mathrm{h}}^{\star} + \rho_{\mathrm{a}}^{\star} v_{\mathrm{a}}^{\star}, \tag{7}$$

$$\rho_{\mathrm{h}}(L,t) v_{\mathrm{h}}(L,t) + \rho_{\mathrm{a}}(L,t) v_{\mathrm{a}}(L,t) = q_{\mathrm{h}}^{\star} + q_{\mathrm{a}}^{\star} + U(t), \tag{8}$$

where the spatial and time domain is defined as $(x,t) \in [0,L] \times \mathbb{R}^{+}$, $\rho_{\mathrm{h}}^{\star}$, $\rho_{\mathrm{a}}^{\star}$ are the equilibrium densities, and $v_{\mathrm{h}}^{\star}$, $v_{\mathrm{a}}^{\star}$ are the equilibrium speed. We will design event-triggered boundary controller boundary control signal of ramp metering or VSL. We define the area occupancy AO to describe the interaction between the two-class vehicles on the road [2], [12]

$$AO(\rho_{\mathrm{h}}, \rho_{\mathrm{a}}) = \frac{a_{\mathrm{h}} \rho_{\mathrm{h}} + a_{\mathrm{a}} \rho_{\mathrm{a}}}{W}, \tag{9}$$

where W is the road width. The impact area for HV a_{h} and AV a_{a} can be described as:

$$a_{\mathrm{h}} = d \times (l + s_{\mathrm{h}}) \tag{10}$$

$$a_{\mathrm{a}} = d \times (l + s_{\mathrm{a}}) \tag{11}$$

where d is the vehicle width, l is the vehicle length. We assume that the vehicle width and length are the same. s_{h} is the car-following gap of HV, s_{a} is the car-following gap of AV. The fundamental diagram based on the area occupancy is introduced for velocity-density equilibrium relation as:

$$v_{\mathrm{h}}^{\star} = V_{e,\mathrm{h}}(\rho_{\mathrm{h}}, \rho_{\mathrm{a}}) = V_{\mathrm{h}} \left(1 - \left(\frac{AO}{\overline{AO}_{\mathrm{h}}}\right)^{\gamma_{\mathrm{h}}}\right) \tag{12}$$

$$v_{\mathrm{a}}^{\star} = V_{e,\mathrm{a}}(\rho_{\mathrm{h}}, \rho_{\mathrm{a}}) = V_{\mathrm{a}} \left(1 - \left(\frac{AO}{\overline{AO}_{\mathrm{a}}}\right)^{\gamma_{\mathrm{a}}}\right) \tag{13}$$

where V_{h}, V_{a} are the maximum speed, $\overline{AO}_{\mathrm{h}}$, $\overline{AO}_{\mathrm{a}}$ are the maximum area occupancy, γ_{h}, γ_{a} are the traffic pressure exponent.

Compared with HV, AV tends to have a larger spacing due to the conservative driving strategies they equipped. A larger spacing leads to a larger impact area, inducing the "creeping effect" on the road that HV can take over AV in congested regimes.

III. Backstepping Control Design

A. Boundary control model

Linearizing the system at its equilibrium point $\rho_{\mathrm{h}}^{\star}$, $\rho_{\mathrm{a}}^{\star}$, $v_{\mathrm{h}}^{\star}$, $v_{\mathrm{a}}^{\star}$ and defining a small deviation $\tilde{\rho}_{\mathrm{h}}(x,t) = \rho_{\mathrm{h}}(x,t) - \rho_{\mathrm{h}}^{\star}$, $\tilde{v}_{\mathrm{h}}(x,t) = v_{\mathrm{h}}(x,t) - v_{\mathrm{h}}^{\star}$, $\tilde{\rho}_{\mathrm{a}}(x,t) = \rho_{\mathrm{a}}(x,t) - \rho_{\mathrm{a}}^{\star}$, $\tilde{v}_{\mathrm{a}}(x,t) = v_{\mathrm{a}}(x,t) - v_{\mathrm{a}}^{\star}$. Writing the system in a augmented expression $\mathbf{z}(x,t) = \begin{bmatrix}\tilde{\rho}_{\mathrm{h}}(x,t) & \tilde{v}_{\mathrm{h}}(x,t) & \tilde{\rho}_{\mathrm{a}}(x,t) & \tilde{v}_{\mathrm{a}}(x,t)\end{bmatrix}^{\mathsf{T}}$ Defining the matrix $\mathbf{V} = \{\hat{v}_{ij}\}_{1 \le i,j \le 4}$ such that the coefficient matrix can be diagonalized as $\mathbf{V}^{-1}\mathbf{J}_{\lambda}\mathbf{V} = \mathrm{Diag}\{\lambda_1, \lambda_2, \lambda_3, \lambda_4\}$, with positive eigenvalues in ascending order. We also define the source term matrix as $\hat{\mathbf{J}} = \mathbf{V}^{-1}\mathbf{J}\mathbf{V} = \{\hat{J}_{ij}\}_{1 \le i,j \le 4}$. The transformation matrix $\mathbf{T}$ is given as

$$\mathbf{T} = \left[\begin{array}{c}\mathbf{T}^{+} \\ \hline \mathbf{T}^{-}\end{array}\right] = \begin{bmatrix} 0 & \mathrm{e}^{-\frac{\hat{J}_{22}}{v_{\mathrm{a}}^{\star}}x} & 0 & 0 \\ 0 & 0 & \mathrm{e}^{-\frac{\hat{J}_{33}}{\lambda_3}x} & 0 \\ \mathrm{e}^{-\frac{\hat{J}_{11}}{v_{\mathrm{h}}^{\star}}x} & 0 & 0 & 0 \\ 0 & 0 & 0 & \mathrm{e}^{-\frac{\hat{J}_{44}}{\lambda_4}x} \end{bmatrix} \mathbf{V}^{-1} \tag{14}$$

where $\mathbf{T}^{+} \in \mathbb{R}^{3\times 4}$ and $\mathbf{T}^{-} \in \mathbb{R}^{1\times 4}$. The change of coordinates is

$$\begin{bmatrix} w_1 & w_2 & w_3 & w_4 \end{bmatrix}^{\mathsf{T}} = \mathbf{T}\mathbf{z}. \tag{15}$$

Then we perform Riemann transformation of the linarized system, thus we get

$$\begin{aligned} \mathbf{w}_t^{+}(x,t) + \Lambda^{+}\mathbf{w}_x^{+}(x,t) =& \Sigma^{++}(x)\mathbf{w}^{+}(x,t) \\ &+ \Sigma^{+-}(x)\mathbf{w}^{-}(x,t), \end{aligned} \tag{16}$$

$$\mathbf{w}_t^{-}(x,t) - \Lambda^{-}\mathbf{w}_x^{-}(x,t) = \Sigma^{-+}(x)\mathbf{w}^{+}(x,t), \tag{17}$$

$$\mathbf{w}^{+}(0,t) = Q\mathbf{w}^{-}(0,t), \tag{18}$$

$$\mathbf{w}^{-}(L,t) = R\mathbf{w}^{+}(L,t) + \bar{U}(t), \tag{19}$$

where $\mathbf{w}^{+} = [w_1, w_2, w_3]^{\mathsf{T}}$, $\mathbf{w}^{-} = w_4$. The coefficient matrices are given as $\Lambda^{+} = \mathrm{Diag}\{\lambda_1, \lambda_2, \lambda_3\}$, $\Lambda^{-} = -\lambda_4$, $\Sigma^{++}(x)$, $\Sigma^{+-}(x)$, $\Sigma^{-+}(x)$, Q, and R are coefficients which can be obtained through Riemann transformation. The details of the coefficients can be found in [2]. Also, $\bar{U}(t) = \mathrm{e}^{-\frac{\hat{J}_{44}}{\lambda_4}L}\frac{1}{\kappa_4}U(t)$, $\kappa_j = v_{\mathrm{h}}^{*}\hat{v}_{1j} + \rho_{\mathrm{h}}^{*}\hat{v}_{2j} + v_{\mathrm{a}}^{*}\hat{v}_{3j} + \rho_{\mathrm{a}}^{*}\hat{v}_{4j}, j = 1,2,3,4$.

B. Free/congestion analysis

It was shown that the eigenvalues satisfying the following condition [21]

$$\lambda_4 \leq \min\{\lambda_1, \lambda_3\} \leq \lambda_2 \leq \max\{\lambda_1, \lambda_3\}. \tag{20}$$

The traffic system can be divided into free and congested regime based on the propagation direction of traffic waves.

- Free regime: the four eigenvalues $\lambda_1 > 0$, $\lambda_2 > 0$, $\lambda_3 > 0$, $\lambda_4 > 0$. Traffic oscillations transport downstream at corresponding speed λ_1, λ_2, λ_3, λ_4. Vehicles can run at their maximum speeds.
- Congested regime: $\lambda_1 > 0$, $\lambda_2 > 0$, $\lambda_3 > 0$, $\lambda_4 < 0$. In the congested regime, the traffic information propagates from downstream to upstream, the efficiency of the traffic system becomes low.

C. Backstepping transformation and controller design

We consider the stabilization of the close-loop system (16)-(19) with continuous control input at each time step. Defining the backstepping transformation:

$$\mathcal{K}\mathbf{w} = \begin{pmatrix} \mathbf{w}^+ \\ \mathbf{w}^- - \int_0^x \mathbf{K}(x,\xi)\mathbf{w}^+(\xi,t) + M(x,\xi)\mathbf{w}^-(\xi,t)d\xi \end{pmatrix} \tag{21}$$

where $\mathbf{w} = [\mathbf{w}^+, \mathbf{w}^-]$ and the backstepping control kernel $\mathbf{K}(x,\xi) \in \mathbb{R}^3$, $M(x,\xi) \in \mathbb{R}^1$ are defined as

$$\mathbf{K}(x,\xi) = \begin{bmatrix} k_1(x,\xi) & k_2(x,\xi) & k_3(x,\xi) \end{bmatrix} \tag{22}$$

Both kernels are defined on the triangular domain $\mathcal{T} = \{0 \leq \xi \leq x \leq L\}$. And the target perturbed system is

$$\begin{aligned} \alpha_t(x,t) + \Lambda^+\alpha_x(x,t) =& \Sigma^{++}(x)\alpha(x,t) + \Sigma^{+-}(x)\beta(x,t) \\ + \int_0^x \mathbf{C}^+(x,\xi)\alpha(\xi,t)d\xi + \int_0^x \mathbf{C}^-(x,\xi)\beta(\xi,t)d\xi, & \quad (23) \\ \beta_t(x,t) - \Lambda^-\beta_x(x,t) = 0, & \quad (24) \\ \alpha(0,t) = Q\beta(0,t) & \quad (25) \\ \beta(L,t) = 0 & \quad (26) \end{aligned}$$

where $\alpha = [\alpha_1, \alpha_2, \alpha_3]^\mathsf{T}$ The coefficients $\mathbf{C}^+(x,\xi) \in \mathbb{R}^{3\times 3}$ and $\mathbf{C}^-(x,\xi) \in \mathbb{R}^{3\times 1}$ are defined on the same triangular domain $\mathcal{T}$. The kernel equations are stated in [2] and the well-posedness of the target system and kernel equations are proved in [9], [22]. The control input is given as

$$\begin{aligned} \bar{U}(t) = \int_0^L \left(\mathbf{K}(L,\xi)\mathbf{w}^+(\xi,t) + M(L,\xi)\mathbf{w}^-(\xi,t)\right)d\xi. \\ - R\mathbf{w}^+(L,t) \end{aligned} \tag{27}$$

D. Inverse Transformation

The transformation (21) is invertible such that the target system share the same properties with the original system. The inverse transformation turn the target system (23)-(26) into the original system (16)-(19):

$$\mathcal{L}\vartheta = \begin{pmatrix} \alpha \\ \beta - \int_0^x (\mathbf{L}(x,\xi)\alpha(\xi,t) + N(x,\xi)\beta(\xi,t))d\xi \end{pmatrix} \tag{28}$$

where $\vartheta = [\alpha_1, \alpha_2, \alpha_3, \beta]^\mathsf{T}$ and $\mathbf{L}(x,\xi) \in \mathbb{R}^3$, $N(x,\xi) \in \mathbb{R}^1$ are definied as

$$\mathbf{L}(x,\xi) = \begin{bmatrix} \ell_1(x,\xi) & \ell_2(x,\xi) & \ell_3(x,\xi) \end{bmatrix} \tag{29}$$

The inverse kernels are also defined on the same triangular domain $\mathcal{T}$. The inverse kernel equations can be easily got in [9]. The states $\mathbf{w}$ and ϑ have equivalent L_2 norms, i.e. there exist two constants $p_1 > 0$ and $p_2 > 0$ such that

$$p_1\|\mathbf{w}\|_{L^2}^2 \leq \|\vartheta\|_{L^2}^2 \leq p_2\|\mathbf{w}\|_{L^2}^2. \tag{30}$$

where $\vartheta = (\alpha_1, \alpha_2, \alpha_3, \beta)$. The continuous-time control input $\bar{U}(t)$ can be calculated using states (α, β) of target system:

$$\begin{aligned} \bar{U}(t) = \int_0^L (\mathbf{L}(L,\xi)\alpha(\xi,t) + N(L,\xi)\beta(\xi,t))d\xi \\ - R\mathbf{w}^+(L,t) \end{aligned} \tag{31}$$

IV. Event-triggered Boundary Control

In this section, we introduce event-triggered conditions for the traffic system which gives the time instant that the controller should update and then ensure the exponential stability of the close-loop system.

First, we consider the stabilization of the closed-loop system on events while sampling the continuous-time controller $\bar{U}(t)$ at certain sequence of time instants and it is updated when the triggering conditions are verified. Then we redefine the boundary control input in (19),

$$\mathbf{w}^-(L,t) = R\mathbf{w}^+(L,t) + \bar{U}_d(t) \tag{32}$$

where $\bar{U}_d(t) = \bar{U}(t) + d(t)$, $\forall t \in [t_k, t_{k+1}), k > 0$. And the $d(t)$ is the deviation of the theoretical control input and the event-triggered control input. And we can get the sampled control law as

$$\begin{aligned} \bar{U}_d(t) = \int_0^L (\mathbf{L}(L,\xi)\alpha(\xi,t_k) + N(L,\xi)\beta(\xi,t_k))d\xi \\ - R\mathbf{w}^+(L,t_k) \end{aligned} \tag{33}$$

thus we get the actuation deviation $d(t)$

$$\begin{aligned} d(t) =& -R(\mathbf{w}^+(L,t_k) - \mathbf{w}^+(L,t)) \\ &+ \int_0^L \Big(\mathbf{L}(L,\xi)(\alpha(\xi,t_k) - \alpha(\xi,t)) \\ &+ N(L,\xi)(\beta(\xi,t_k) - \beta(\xi,t)\Big)d\xi \end{aligned} \tag{34}$$

Applying the sampled control law $\bar{U}_d(t)$ to the system (16) - (19), we get the pertubed target system

$$\begin{aligned} \alpha_t(x,t) + \Lambda^+\alpha_x(x,t) =& \Sigma^{++}(x)\alpha(x,t) + \Sigma^{+-}(x)\beta(x,t) \\ + \int_0^x \mathbf{C}^+(x,\xi)\alpha(\xi,t)d\xi + \int_0^x \mathbf{C}^-(x,\xi)\beta(\xi,t)d\xi, & \quad (35) \\ \beta_t(x,t) - \Lambda^-\beta_x(x,t) = 0, & \quad (36) \\ \alpha(0,t) = Q\beta(0,t), & \quad (37) \\ \beta(L,t) = d(t). & \quad (38) \end{aligned}$$

We consider a triggering condition relies on the evolution of $d(t)$ and the following Lyapunov function,

$$V(t) = \int_0^L \sum_{i=1}^{3} \frac{A_i}{\lambda_i} \mathrm{e}^{-\frac{\mu x}{\lambda_i}} \alpha_i^2(x,t) + \frac{B}{\Lambda^-} \mathrm{e}^{\frac{\mu x}{\Lambda^-}} \beta^2(x,t) dx \tag{39}$$

where the constant coefficients A_1, A_2, A_3, B and μ are positive. The Lyapunov candidate is equivalent to the L_2 norm of the state ϑ, therefore, there exist two constants $p_3 > 0$ and $p_4 > 0$ such that

$$p_3 \|\vartheta\|_{L^2}^2 \leq V(t) \leq p_4 \|\vartheta\|_{L^2}^2. \tag{40}$$

A. Dynamic triggering condition

We define the event-triggered mechanism (ETM) using the dynamic triggering condition which can be derived by the evolution of the controller deviation (34) and another dynamic variable $m(t)$.

Definition 1. *Let the Lyapunov candidate $V(t)$ be given by* (39)*. The event-triggered controller is defined in* (33) *with a dynamic event-triggered mechanism. The time of the execution $t_k \geq 0$ from $t_0 = 0$ in a finite number set of times. The set is determined by:*

- *if $\{t > t_k \wedge \zeta B \mathrm{e}^{\frac{\mu L}{\Lambda^-}} d^2(t) \geq \zeta\mu\sigma V(t) - m(t)\} = \emptyset$, then the set of the times of the events is $\{ t_0, \ldots, t_k\}$.*
- *if $\{t > t_k \wedge \zeta B \mathrm{e}^{\frac{\mu L}{\Lambda^-}} d^2(t) \geq \zeta\mu\sigma V(t) - m(t)\} \neq \emptyset$, then the next execution time is determined by: $t_{k+1} = \inf\{t > t_k \wedge B \mathrm{e}^{\frac{\mu L}{\Lambda^-}} d^2(t) \geq \zeta\mu\sigma V(t) - m(t)\}$,*

where $m(t)$ satisfies the ordinary differential equation,

$$\begin{aligned} \dot{m}(t) = &- \eta m(t) + B \mathrm{e}^{\frac{\mu L}{\Lambda^-}} d^2(t) - \sigma\mu V(t) \\ &- \sum_{i=1}^{3} \varsigma_i \alpha_i^2(L,t) - \varsigma_4 \beta^2(0,t), \end{aligned} \tag{41}$$

where $\zeta > 0$, $\mu > 0$, $\sigma > 0$, $\varsigma_i > 0$, $i \in \{1,2,3,4\}$, $\eta > 0$ and $m(0) = m^0$.

Based on the definition 1, we have the following result for $m(t)$.

Lemma 2. *Under the ETM in Definition 1, it holds that $\zeta B \mathrm{e}^{\frac{\mu L}{\Lambda^-}} d^2(t) - \zeta\mu\sigma V(t) + m(t) \leq 0$ with $m(t) \leq 0$*

Proof. We already know the ETM in Definition 1. It holds that the system in the simulation period always guarantee the following condition,

$$\zeta B \mathrm{e}^{\frac{\mu L}{\Lambda^-}} d^2(t) - \zeta\mu\sigma V(t) \leq -m(t). \tag{42}$$

We have the result

$$B \mathrm{e}^{\frac{\mu L}{\Lambda^-}} d^2(t) - \mu\sigma V(t) \leq -\frac{1}{\zeta} m(t), \tag{43}$$

using (41), we get

$$\dot{m}(t) \leq -\eta m - \frac{1}{\zeta} m(t) - \sum_{i=1}^{3} \varsigma_i \alpha_i^2(L,t) - \varsigma_4 \beta^2(0,t). \tag{44}$$

Using the comparison principle, we have

$$m(t) \leq 0, \forall t \geq 0, \tag{45}$$

this finishes the proof of Lemma 2. □

We also have the following lemma for the boundness of the actuation deviation $d(t)$.

Lemma 3. *There exists $\epsilon_i > 0, i \in \{1,2,3\}$, ϕ_1 and $\phi_2 > 0$, for the $d(t)$ introduced in* (34) *with $t \in (t_k, t_{k+1})$, such that*

$$\dot{d^2}(t) \leq \sum_{i=1}^{3} \epsilon_i \alpha_i^2(L,t) + \phi_1 d^2(t) + \phi_2 V(t). \tag{46}$$

Proof. Taking time derivative of $d(t)$, we have

$$\dot{d}(t) = -\int_0^L \mathbf{L}(L,\xi)\alpha_t(\xi,t) + N(L,\xi)\beta_t(\xi,t) d\xi. \tag{47}$$

Using the dynamics of the perturbed target system in (35) - (38) and integrating by parts, we get

$$\begin{aligned} \dot{d}(t) = &\mathbf{L}(L,L)\Lambda^+\alpha(L,t) - N(L,L)\Lambda^-\beta(L,t) \\ &+ \left(N(L,0)\Lambda^- - \mathbf{L}(L,0)\Lambda^+ Q\right)\beta(0,t) \\ &- \int_0^L \mathbf{L}_\xi(L,\xi)\Lambda^+\alpha(\xi,t)d\xi + \int_0^L N_\xi(L,\xi)\Lambda^-\beta(\xi,t)d\xi \\ &- \int_0^L \mathbf{L}(L,\xi)\Sigma^{++}(\xi)\mathbf{w}^+(\xi,t)d\xi \\ &- \int_0^L \mathbf{L}(L,\xi)\Sigma^{+-}(\xi)\mathbf{w}^-(\xi,t)d\xi. \end{aligned} \tag{48}$$

Taking the square of $\dot{d}(t)$, combining Young's inequality, we have

$$\begin{aligned} \dot{d^2}(t) \leq &2(\mathbf{L}(L,L)\Lambda^+\alpha(L,t) - N(L,L)\Lambda^-\beta(L,t))^2 \\ &+ 2\left(-\int_0^L \mathbf{L}_\xi(L,\xi)\Lambda^+\alpha(\xi,t) - N_\xi(L,\xi)\Lambda^-\beta(\xi,t)d\xi \right. \\ &- \int_0^L \mathbf{L}(L,\xi)\Sigma^{++}(\xi)\mathbf{w}^+(\xi,t)d\xi \\ &\left. - \int_0^L \mathbf{L}(L,\xi)\Sigma^{+-}(\xi)\mathbf{w}^-(\xi,t)d\xi\right)^2. \end{aligned} \tag{49}$$

Using Cauchy-Schwarz inequality, we get

$$\begin{aligned} \dot{d^2}(t) \leq &8\sum_{i=1}^{3} \ell_i^2(L,L)\lambda_i^2\alpha_i^2(L,t) \\ &+ 8N^2(L,L)(\Lambda^-)^2\beta^2(L,t) + \frac{8}{p_3}c_1 V(t) + \frac{8}{p_1 p_3}c_2 V(t) \\ \leq &8\sum_{i=1}^{3} \ell_i^2(L,L)\lambda_i^2\alpha_i^2(L,t) + 8N^2(L,L)(\Lambda^-)^2 d^2(t) \\ &+ \frac{8}{p_3}\left(c_1 + \frac{c_2}{p_1}\right)V(t), \end{aligned} \tag{50}$$

where $c_1 = \max\{\int_0^L (\mathbf{L}_\xi(L,\xi)\Lambda^+)^2 d\xi, \int_0^L (N_\xi(L,\xi)\Lambda^-)^2 d\xi\}$ $c_2 = \max\{\int_0^L (\mathbf{L}(L,\xi)\Sigma^{++}(\xi))^2 d\xi, \int_0^L (\mathbf{L}(L,\xi)\Sigma^{+-}(\xi))^2 d\xi\}$. And thus we get that

$\epsilon_i = 8\ell_i^2(L,L)\lambda_i, i \in \{1,2,3\}$, $\phi_1 = 8N^2(L,L)(\Lambda^-)^2$, $\phi_2 = \frac{8}{p_3}\left(c_1 + \frac{c_2}{p_1}\right)$. This concludes the proof of Lemma 3. □

B. Avoidance of Zeno phenomenon

Under the dynamic event triggering condition, the Zeno phenomenon should be avoided. In this section, we prove the dynamic event triggering condition for the system (16) - (19) avoids the Zeno phenomenon. We have the following theorem.

Theorem 4. *There exists a minimal dwell-time $\tau^\star > 0$ between two adjacent triggering times, $t_{k+1} - t_k \geq \tau^\star, k \geq 0$, under the dynamic triggering condition in Definition 1 with parameters ζ, μ, σ, $\varsigma_i, i \in \{1,2,3,4\}$, η, $\epsilon_i, i \in \{1,2,3\}$. And the parameters satisfying:*

$$\varsigma_i \geq \max\{\zeta B\mathrm{e}^{\frac{\mu L}{\Lambda^-}}\epsilon_i, \zeta\mu\epsilon_i, i \in \{1,2,3\}\} \tag{51}$$

$$\varsigma_4 \geq \max\{0, -2\zeta\mu(\sum A_i q_i^2 - B), i \in \{1,2,3\} \tag{52}$$

Proof. We know from the Definition 1 that for all time $t \geq 0$, all events are executed to guarantee

$$\zeta B\mathrm{e}^{\frac{\mu L}{\Lambda^-}} d^2(t) \leq \zeta\mu\sigma V(t) - m(t). \tag{53}$$

Then we define the following function

$$\Psi(t) = \frac{\zeta B\mathrm{e}^{\frac{\mu L}{\Lambda^-}} d^2(t) + \frac{1}{2}m(t)}{\zeta\mu\sigma V - \frac{1}{2}m(t)}. \tag{54}$$

The function $d(t)$ and $V(t)$ are continuous on time interval $[t_k, t_{k+1}]$, so that the function $\Psi(t)$ is also a continuous function at $[t_k, t_{k+1}]$. We can derive that there exists $t_k' > t_k$ such that $\forall t \in [t_k', t_{k+1}]$, $\Psi(t) \in [0,1]$ using the intermediate value theorem. Taking time derivative to the function $\Psi(t)$, we get

$$\dot{\Psi}(t) = \frac{2\zeta B\mathrm{e}^{\frac{\mu L}{\Lambda^-}} d\dot{d} + \frac{1}{2}\dot{m}}{\zeta\mu\sigma V - \frac{1}{2}m} - \frac{\zeta\sigma\mu\sigma\dot{V} - \frac{1}{2}\dot{m}}{\zeta\mu\sigma V - \frac{1}{2}m}\Psi. \tag{55}$$

Using Young inequality, we have

$$\begin{aligned}
\dot{\Psi}(t) \leq\ & \frac{\zeta B\mathrm{e}^{\frac{\mu L}{\Lambda^-}} d^2}{\zeta\mu\sigma V - \frac{1}{2}m} + \frac{\zeta B\mathrm{e}^{\frac{\mu L}{\Lambda^-}} \dot{d}^2}{\zeta\mu\sigma V - \frac{1}{2}m} \\
&+ \frac{\frac{1}{2}(-\eta m + B\mathrm{e}^{\frac{\mu L}{\Lambda^-}} d^2 - \sigma\mu V)}{\zeta\sigma\mu V - \frac{1}{2}m} \\
&+ \frac{\frac{1}{2}\left(-\sum_{i=1}^3 \varsigma_i\alpha_i^2(L,t) - \varsigma_4\beta^2(0,t)\right)}{\zeta\mu\sigma V - \frac{1}{2}m} - \frac{\zeta\mu\dot{V}\Psi}{\zeta\mu\sigma V - \frac{1}{2}m} \\
&+ \frac{\frac{1}{2}\left(-\eta m + B\mathrm{e}^{\frac{\mu L}{\Lambda^-}} d^2 - \sigma\mu V\right)}{\zeta\mu\sigma V - \frac{1}{2}m}\Psi \\
&+ \frac{\frac{1}{2}\left(-\sum_{i=1}^3 \varsigma_i\alpha_i^2(L,t) - \varsigma_4\beta^2(0,t)\right)}{\zeta\mu\sigma V - \frac{1}{2}m}\Psi.
\end{aligned} \tag{56}$$

As defined in (39), the time derivative of $V(t)$ can be gotten by integrating by parts and using boundary conditions of perturbed target system. Thus the $\dot{V}$ is given as

$$\begin{aligned}
\dot{V} \leq & -\sum_{i=1}^3 A_i\mathrm{e}^{-\frac{\mu L}{\lambda_i}}\alpha_i^2(L,t) + (\sum_{i=1}^3 A_i q_i^2 - B)\beta^2(0,t) \\
& + B\mathrm{e}^{\frac{\mu L}{\Lambda^-}} d^2(t) - (\mu - \gamma)V,
\end{aligned} \tag{57}$$

where $\gamma = \frac{2A}{p_3 \min\{\lambda_i\}}(\max_{x\in[0,L]} \|\Sigma^{++}(x)\| + (1 + \frac{1}{p_1}) \max_{x\in[0,L]} \|\Sigma^{+-}(x)\|)$.

$$\dot{V} \leq -\sum_{i=1}^3 \alpha_i^2(L,t) + \beta^2(0,t) + B\mathrm{e}^{\frac{\mu L}{\Lambda^-}} d^2(t) - (\mu - \gamma)V, \tag{58}$$

Replacing $\dot{V}$ and using (3), we have

$$\begin{aligned}
\dot{\Psi}(t) \leq & -\frac{(\zeta\mu(\sum A_i q_i^2 - B) + \frac{1}{2}\varsigma_4)\beta^2(0,t)}{\zeta\mu\sigma V - \frac{1}{2}m}\Psi \\
& - \frac{\frac{1}{2}\eta m}{\zeta\mu\sigma V - \frac{1}{2}m}\Psi + \frac{\sum(\zeta\mu\epsilon_i - \varsigma_i)\alpha_i^2(L,t)}{\zeta\mu\sigma V - \frac{1}{2}m}\Psi \\
& + \frac{B\mathrm{e}^{\frac{\mu L}{\Lambda^-}} d^2(-\zeta\mu\sigma + \frac{1}{2})}{\zeta\mu\sigma V - \frac{1}{2}m}\Psi + \frac{(\zeta\mu\sigma(\mu - \gamma) - \frac{1}{2}\mu\sigma)V}{\zeta\mu\sigma V - \frac{1}{2}m}\Psi \\
& + \frac{\zeta B\mathrm{e}^{\frac{\mu L}{\Lambda^-}}(1 + \phi_1 + \frac{1}{2\zeta})d^2}{\zeta\mu\sigma V - \frac{1}{2}m} + \frac{\sum(\zeta B\mathrm{e}^{\frac{\mu L}{\Lambda^-}}\epsilon_i - \varsigma_i)\alpha_i^2(L,t)}{\zeta\mu\sigma V - \frac{1}{2}m} \\
& + \frac{(\zeta B\mathrm{e}^{\frac{\mu L}{\Lambda^-}}\phi_2 - \frac{1}{2}\mu\sigma)V}{\zeta\mu\sigma V - \frac{1}{2}m} - \frac{\frac{1}{2}\eta m}{\zeta\mu\sigma V - \frac{1}{2}m} - \frac{\frac{1}{2}\varsigma_4\beta^2(0,t)}{\zeta\mu\sigma V - \frac{1}{2}m}
\end{aligned} \tag{59}$$

Choosing $\varsigma_i \geq \zeta B\mathrm{e}^{\frac{\mu L}{\Lambda^-}}\epsilon_i$ and $\varsigma_i \geq \zeta\mu\epsilon_i$, $i \in \{1,2,3\}$, $\varsigma_4 > 0$ and $\varsigma_4 + 2\zeta\mu(\sum A_i q_i^2 - B) > 0$, we get the following equation after simplification

$$\begin{aligned}
\dot{\Psi}(t) \leq & \frac{\zeta B\mathrm{e}^{\frac{\mu L}{\Lambda^-}}(1 + \phi_1 + \frac{1}{2\zeta})d^2}{\zeta\mu\sigma V - \frac{1}{2}m} + \frac{(\zeta B\mathrm{e}^{\frac{\mu L}{\Lambda^-}}\phi_2 - \frac{1}{2}\mu\sigma)}{\zeta\mu\sigma} + \eta \\
& + \frac{B\mathrm{e}^{\frac{\mu L}{\Lambda^-}} d^2(-\zeta\mu\sigma + \frac{1}{2})}{\zeta\mu\sigma V - \frac{1}{2}m}\Psi + \eta\Psi + \frac{(\zeta\mu\sigma(\mu - \gamma) - \frac{1}{2}\mu\sigma)}{\zeta\mu\sigma}\Psi
\end{aligned} \tag{60}$$

Rewriting the equation, thus it can be deduced that

$$\begin{aligned}
\dot{\Psi}(t) \leq & \frac{(\zeta B\mathrm{e}^{\frac{\mu L}{\Lambda^-}} d^2 + \frac{1}{2}m - \frac{1}{2}m)(1 + \phi_1 + \frac{1}{2\zeta})}{\zeta\mu\sigma V - \frac{1}{2}m} \\
& + \eta + \frac{(\zeta B\mathrm{e}^{\frac{\mu L}{\Lambda^-}} d^2 + \frac{1}{2}m - \frac{1}{2}m)(-\zeta\mu + \frac{1}{2})}{\zeta(\zeta\mu\sigma V - \frac{1}{2}m)}\Psi + \eta\Psi \\
& + \frac{(\zeta\mu(\mu - \gamma) - \frac{1}{2}\mu\sigma)}{\zeta\mu\sigma}\Psi + \frac{(\zeta B\mathrm{e}^{\frac{\mu L}{\Lambda^-}}\phi_2 - \frac{1}{2}\mu)}{\zeta\mu\sigma}.
\end{aligned} \tag{61}$$

Rearranging the above equation, thus we have

$$\begin{aligned}
\dot{\Psi}(t) \leq & \left(\frac{-\zeta\mu + \frac{1}{2}}{\zeta}\right)\Psi^2 + \left(1 + \phi_1 + \frac{1}{2\zeta}\right. \\
& \left. + \frac{-\zeta\mu\sigma + \frac{1}{2}}{\zeta} + \eta + \frac{\zeta\mu\sigma(\mu - \gamma) - \frac{1}{2}\mu\sigma}{\zeta\mu\sigma}\right)\Psi
\end{aligned}$$

$$+\left(\frac{(\zeta B\mathrm{e}^{\frac{\mu L}{\Lambda^-}}\phi_2-\frac{1}{2}\mu\sigma)}{\zeta\mu\sigma}+\eta+1+\phi_1+\frac{1}{2\zeta}\right). \tag{62}$$

Thus the $\Psi(t)$ has the form

$$\Psi(t)\leq\varphi_1\Psi^2(t)+\varphi_2\Psi(t)+\varphi_3 \tag{63}$$

where $\varphi_1=\frac{1}{2\zeta}-\mu\sigma$, $\varphi=1+\phi_1+\frac{1}{2\zeta}(1-\sigma)\mu-\gamma+\eta$, $\varphi_3=\frac{B\mathrm{e}^{\frac{\mu L}{\Lambda^-}}\phi_2}{\mu\sigma}+1+\eta+\phi_1$. Using the comparison principle, we get the time from $\Psi(t_k')=0$ to $\Psi(t_{k+1})=1$ is at least

$$\tau^\star=\int_0^L\frac{1}{\varphi_1 s^2+\varphi_2 s+\varphi_3}ds. \tag{64}$$

Then, $t_{k+1}-t_k\geq t_{k+1}-t_{t_k'}=\tau^\star$. This finishes the proof of Theorem 4. □

Now that have proved that there exists a minimal dwell time between two adjacent events. The Zeno phenomenon is avoided. Based on the previous results, the exponential stability of the system (16) - (19) with the event-triggered controller (33) was obtained, as stated in Theorem 5.

Theorem 5. *Let* $A_i>0, i\in\{1,2,3\}$, $B>0$, $\zeta>0$, $\eta\in(0,1)$, $\varsigma_i, i\in\{1,2,3,4\}\in(0,1)$ *such that*

$$\varsigma_i-A_i\mathrm{e}^{-\frac{\mu L}{\lambda_i}}\leq 0, i\in\{1,2,3\} \tag{65}$$

$$\varsigma_4+\sum_{i=1}^{3}A_iq_i^2-B\leq 0, i\in\{1,2,3\} \tag{66}$$

V is given by (39) *and d is given by* (34). *The system* (16)-(19) *with the event-triggered controller* (33) *is exponential stable under the ETM in Definition 1.*

Proof. We consider the following Lyapunov candidate for perturbed target system (35) - (38),

$$V_d(t,m)=V(t)-m(t) \tag{67}$$

Taking time derivative of the Lyapunov candidate, we get

$$\begin{aligned}\dot V_d(t,m)\leq& B\mathrm{e}^{\frac{\mu L}{\Lambda^-}}d^2(t)-(\mu-\gamma)V-\dot m(t)\\&-\sum_{i=1}^{3}A_i\mathrm{e}^{-\frac{\mu L}{\lambda_i}}\alpha_i^2(L,t)+(\sum_{i=1}^{3}A_iq_i^2-B)\beta^2(0,t),\end{aligned} \tag{68}$$

taking into the expression of $\dot m(t)$, we get

$$\begin{aligned}\dot V_d\leq&-(\mu-\gamma)V+B\mathrm{e}^{\frac{\mu L}{\Lambda^-}}d^2(t)+\eta m+\mu\sigma V\\&-B\mathrm{e}^{\frac{\mu L}{\Lambda^-}}d^2(t)+\sum_{i=1}^{3}(\varsigma_i-A_i\mathrm{e}^{-\frac{\mu L}{\lambda_i}})\alpha_i^2(L,t)\\&+(\varsigma_4+\sum_{i=1}^{3}A_iq_i^2-B)\beta^2(0,t).\end{aligned} \tag{69}$$

Simplifying the equation, thus

$$\dot V_d\leq-(\mu(1-\sigma)-\gamma)V_d+(\eta-(\mu(1-\sigma)-\gamma))m. \tag{70}$$

Choosing $\eta-(\mu(1-\sigma)-\gamma)\geq 0$, we get

$$\dot V_d\leq-(\mu(1-\sigma)-\gamma)V_d. \tag{71}$$

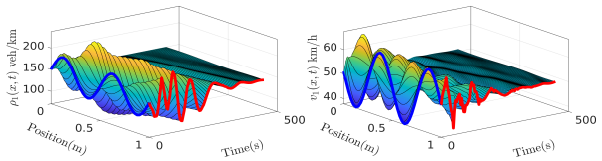

(a) HV

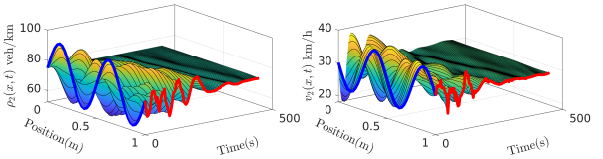

(b) AV

Fig. 1: The density and velocity under event-triggered controller with spacing $s_\mathrm{a}=16$m

Using comparison principle again and $m(0)=0$, thus

$$\dot V(t)\leq\mathrm{e}^{(-(\mu(1-\sigma)-\gamma)t)}V(0) \tag{72}$$

This concludes the proof of Theorem 5. □

V. Numerical Simulation

In this section, we provide the numerical simulation for the closed-loop system with event-triggered controller. Taking the equilibrium density as $\rho_\mathrm{h}^\star=150$veh/km, $\rho_\mathrm{a}^\star=75$veh/km, such that $v_\mathrm{h}^\star=29.16$km/h, $v_\mathrm{a}^\star=13.32$veh/km can be calculated by the fundamental diagram. The relaxation time is set as $\tau_\mathrm{h}=30$s, $\tau_\mathrm{a}=60$s. The pressure exponent value is selected as $\gamma_\mathrm{h}=2.5$, $\gamma_\mathrm{a}=2$. The car-following gap are $s_\mathrm{h}=5$m, $s_\mathrm{a}=16$m. The maximum area occupancy $\overline{AO}_\mathrm{h}=0.9$, $\overline{AO}_\mathrm{a}=0.85$ In addition, we choose $\zeta=8\times10^{-3}$, $\sigma=1\times10^{-4}$, $\eta=0.9$, $A_1=2\times10^{-2}$, $A_2=3\times10^{-3}$, $A_3=4\times10^{-3}$, $B=9\times10^{-3}$, and we also choose $\varrho_1=2\times10^{-10}$, $\varrho_2=2\times10^{-9}$, $\varrho_3=1.2\times10^{-12}$, $\varsigma_4=0.01$, $\mu=5\times10^{-4}$. We run the simulation on a $L=1000$m long road whose width is 6m and the simulation time is 450s.

The closed-loop results of the mixed traffic system under the event-triggered controller is shown in Fig. 1. Fig. 1a represents the density and velocity of the HV while Fig. 1b denotes AV. It can be observed that the event-triggered controller can stabilize the mixed-autonomy traffic system. We also provide the comparison between the continuous controller using backstepping method and the event-triggered controller in Fig. 2a. The traffic management system do not need to update the control input at each time-step by using the event-triggered controller, therefore, the computational burden has been reduced. The triggered times and the release time interval are plotted in Fig. 2b. The maximum release time interval is 22 seconds meaning that we do not need to recompute the control input and just use the previous control input. The triggered times in the whole simulation period is 165.

We then test the different spacing settings of AV, we run the simulation with spacing of AV $s_\mathrm{a}=20$m. The

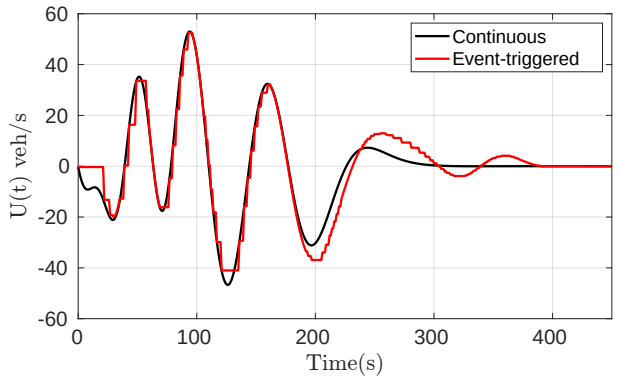

(a) The control input between continuous controller and event-triggered controller

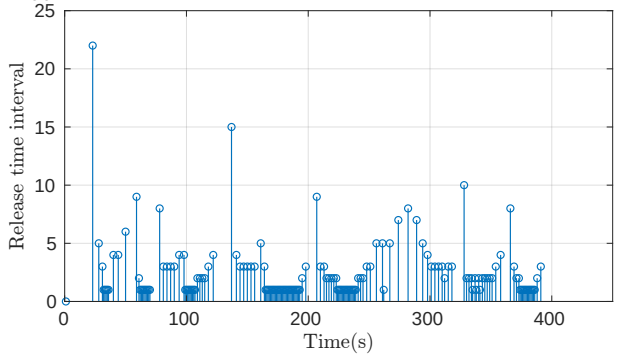

(b) Release instants under the event-triggered controller

Fig. 2: The performance of event-triggered controller with spacing $s_{\mathrm{a}} = 16\mathrm{m}$

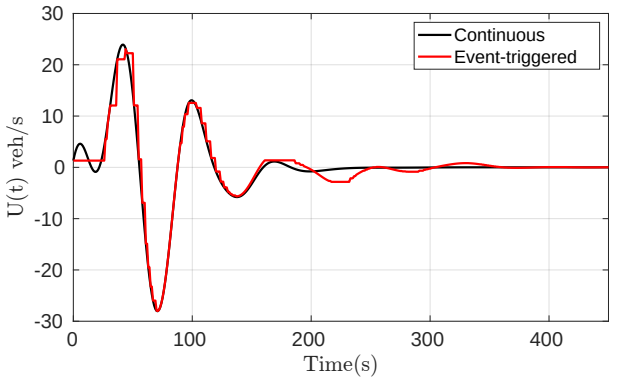

(a) The control input between continuous controller and event-triggered controller

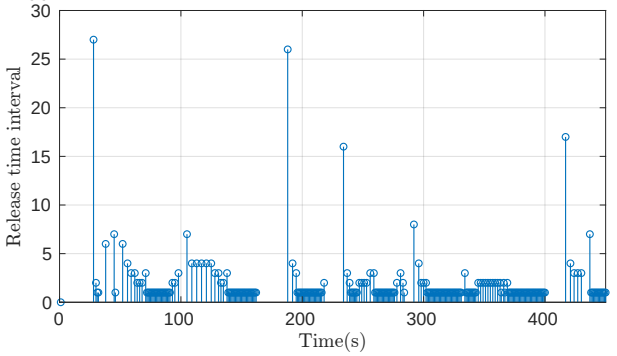

(b) Release instants under the event-triggered controller

Fig. 3: The performance of event-triggered controller with spacing $s_{\mathrm{a}} = 20\mathrm{m}$

comparison between the continuous controller and event-triggered controller is shown in Fig. 3a. The triggered times and the release time interval are plotted in Fig. 3b. The maximum release time interval is 27s and the triggered times is 244. Results show the traffic system tends to become more congested with a larger spacing of AV. The event triggered controller must need to execute more times to make the system stable.

VI. CONCLUSIONS

The event-triggered control of mixed-autonomy traffic system consisting both HV and AV is investigated. The traffic dynamics of mixed-autonomy traffic system is represented by an extend-ARZ model. The backstepping controller is designed to stabilize the system and then the dynamic ETM is defined. The event-triggered boudary controller is derived through the dynamic ETM. And the Lyapunov analysis is applied to derive the stability results of the mixed-autonomy system with event-triggered controller. A numerical simulation is conducted to illustrate the effect of event-triggered controller. The future work will focus on developing the observer-based event-triggered controller for the mixed-autonomy traffic system.

REFERENCES

[1] A. Aw and M. Rascle. Resurrection of "second order" models of traffic flow. *SIAM journal on applied mathematics*, 60(3):916–938, 2000.

[2] M. Burkhardt, H. Yu, and M. Krstic. Stop-and-go suppression in two-class congested traffic. *Automatica*, 125:109381, 2021.

[3] N. Espitia, J. Auriol, H. Yu, and M. Krstic. Traffic flow control on cascaded roads by event-triggered output feedback. *International Journal of Robust and Nonlinear Control*, 32(10):5919–5949, 2022.

[4] N. Espitia, A. Girard, N. Marchand, and C. Prieur. Event-based control of linear hyperbolic systems of conservation laws. *Automatica*, 70:275–287, 2016.

[5] A. Ferrara, S. Sacone, and S. Siri. Event-triggered model predictive schemes for freeway traffic control. *Transportation Research Part C: Emerging Technologies*, 58:554–567, 2015.

[6] A. Girard. Dynamic triggering mechanisms for event-triggered control. *IEEE Transactions on Automatic Control*, 60(7):1992–1997, 2014.

[7] P. Goatin, S. Göttlich, and O. Kolb. Speed limit and ramp meter control for traffic flow networks. *Engineering Optimization*, 48(7):1121–1144, 2016.

[8] G. Gomes and R. Horowitz. Optimal freeway ramp metering using the asymmetric cell transmission model. *Transportation Research Part C: Emerging Technologies*, 14(4):244–262, 2006.

[9] L. Hu, F. Di Meglio, R. Vazquez, and M. Krstic. Control of homodirectional and general heterodirectional linear coupled hyperbolic PDEs. *IEEE Transactions on Automatic Control*, 61(11):3301–3314, 2016.

[10] I. Karafyllis and M. Papageorgiou. Feedback control of scalar conservation laws with application to density control in freeways by means of variable speed limits. *Automatica*, 105:228–236, 2019.

[11] M. J. Lighthill and G. B. Whitham. On kinematic waves ii. a theory of traffic flow on long crowded roads. *Proceedings of the Royal Society of London. Series A. Mathematical and Physical Sciences*, 229(1178):317–345, 1955.

[12] R. Mohan and G. Ramadurai. Heterogeneous traffic flow modelling using second-order macroscopic continuum model. *Physics Letters A*, 381(3):115–123, 2017.

[13] C. Pasquale, S. Sacone, S. Siri, and A. Ferrara. Hierarchical centralized/decentralized event-triggered control of multiclass traf-

fic networks. *IEEE Transactions on Control Systems Technology*, 29(4):1549–1564, 2020.

[14] P. I. Richards. Shock waves on the highway. *Operations research*, 4(1):42–51, 1956.

[15] S. Siri, C. Pasquale, S. Sacone, and A. Ferrara. Freeway traffic control: A survey. *Automatica*, 130:109655, 2021.

[16] P. Tabuada. Event-triggered real-time scheduling of stabilizing control tasks. *IEEE Transactions on Automatic control*, 52(9):1680–1685, 2007.

[17] H. Yu, J. Auriol, and M. Krstic. Simultaneous downstream and upstream output-feedback stabilization of cascaded freeway traffic. *Automatica*, 136:110044, 2022.

[18] H. Yu and M. Krstic. Traffic congestion control for Aw–Rascle–Zhang model. *Automatica*, 100:38–51, 2019.

[19] H. M. Zhang. A non-equilibrium traffic model devoid of gas-like behavior. *Transportation Research Part B: Methodological*, 36(3):275–290, 2002.

[20] L. Zhang and C. Prieur. Stochastic stability of markov jump hyperbolic systems with application to traffic flow control. *Automatica*, 86:29–37, 2017.

[21] P. Zhang, R.-X. Liu, S. Wong, and S.-Q. Dai. Hyperbolicity and kinematic waves of a class of multi-population partial differential equations. *European Journal of Applied Mathematics*, 17(2):171–200, 2006.

[22] Y. Zhang, H. Yu, J. Auriol, and M. Pereira. Mean-square exponential stabilization of mixed-autonomy traffic PDE system. *arXiv preprint arXiv:2310.15547*, 2023.